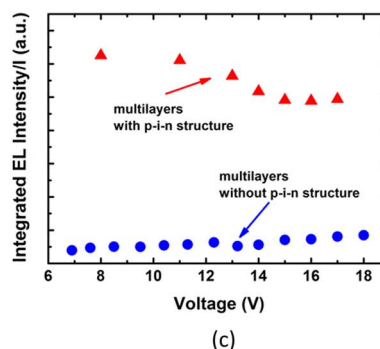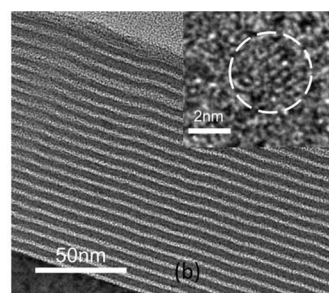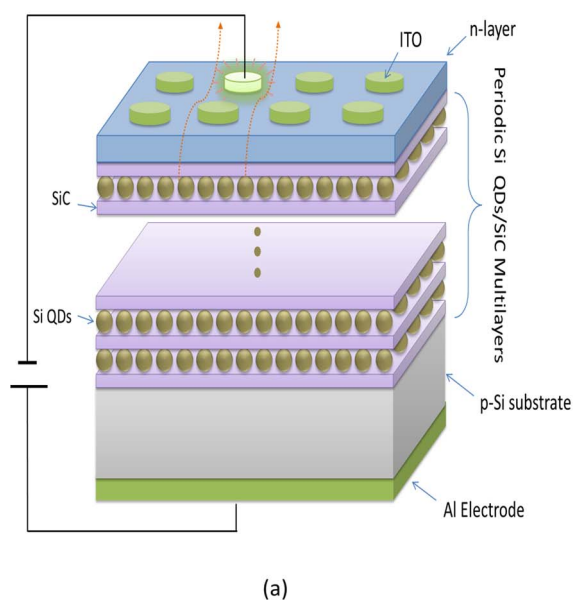# Electroluminescence Devices Based on Si Quantum Dots/SiC Multilayers Embedded in PN Junction

Volume 6, Number 1, February 2014

X. Xu
Y. Q. Cao
P. Lu
J. Xu, Member, IEEE
W. Li
K. J. Chen

♦IEEE

Electroluminescence Devices Based on Si Quantum Dots/SiC Multilayers Embedded in PN Junction

X. Xu, Y. Q. Cao, P. Lu, J. Xu, *Member, IEEE*, W. Li, and K. J. Chen

School of Electronics Science and Engineering and National Laboratory of Solid State Microstructures, Nanjing University, Nanjing 210093, China

Abstract: We deposited a p-i-n structure device with alternative amorphous Si (a-Si) and amorphous SiC (a-SiC) multilayers as an intrinsic layer in a plasma-enhanced chemical vapor deposition (PECVD) system. A KrF pulsed excimer laser-induced crystallization of a-Si/a-SiC stacked structures was used to prepare Si quantum dots (Si QDs)/SiC multilayers. The formation of Si QDs with an average size of 4 nm was confirmed by Raman spectra, whereas the layered structures were revealed by cross-sectional transmission electron microscopy. Electroluminescence (EL) devices containing Si QDs/SiC multilayers embedded in a p-n junction were fabricated, and the device performance was studied and compared with the reference device without the p-i-n structure. It was found that the turn-on voltage was reduced and that luminescence efficiency was significantly enhanced by using the p-i-n device structure. The recombination mechanism of carriers in a Si-QD-based EL device was also discussed, and the improved device performance can be attributed to the enhanced radiative recombination probability in a p-i-n EL device.

Index Terms: Light-emitting diodes, silicon nanophotonics, synthesis and fabrication methods.

1. Introduction

A silicon-based light emitter is one of the crucial devices in realizing Si-based monolithic opto-electronic integration, which has the advantages of high speed and low power consumption [1]–[3]. Recently, Si quantum dots (Si QDs) embedded in an amorphous SiO_2, SiN, or SiC host matrix have attracted much attention since they can emit intense luminescence both under optical and electronic excitation at room temperature [4]–[9]. It has been reported that the radiative recombination probability can be significantly enhanced in Si QDs compared with their bulk counterpart due to the enhanced overlapping of electron and hole wave functions in a confined system [10]–[13].

In our previous works, Si QDs/SiC multilayers were fabricated by thermal annealing of amorphous Si (a-Si)/amorphous SiC (a-SiC) stacked structures at high temperature ($> 900\ °C$). Electroluminescence (EL) devices were fabricated by using a metal/(Si QDs/SiC) MLs/p-Si structure. The size-dependent EL characteristics were observed, which suggested that the origin of luminescence in Si QDs/SiC multilayers (MLs) can be attributed to the quantum confinement effect, which is different from that in Si QDs/SiO_2 MLs, in which the interface states played an important role in the
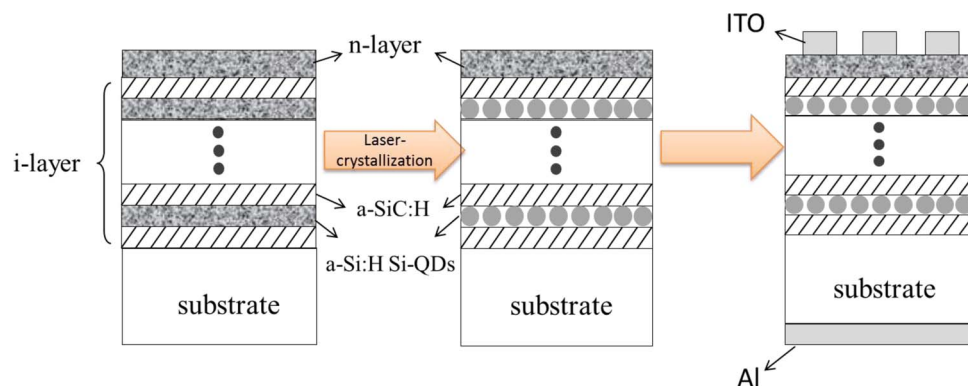
Fig. 1. The schematic diagrams of EL device fabrication process.

recombination process [12], [14]. However, the emission intensity at the present stage is still low, and the output light power is on the order of several picowatts. In order to further improve the emission efficiency, one of the possible ways is to utilize the p-n or the p-i-n junction structure to promote the carrier injection and recombination probability [14], [15].

In the present work, we propose the KrF pulsed excimer laser crystallization technique to prepare Si QDs/SiC MLs embedded in the p-n junction to get a p-i-n EL device structure. The laser crystallization technique can get size-controllable sizes without inducing the series impurities inter-diffusion problem as reported in the high-temperature annealing process [16]. We show that the good rectification characteristics can be achieved in our EL device indicating the formation of a p-i-n junction after laser crystallization. It is found that the EL intensity can be obviously improved and that the turn-on voltage of the device is reduced compared with the device without the p-i-n structure. The power-low of EL intensity as a function of injunction current indicates that the radiative recombination is enhanced by forming the p-i-n device structure.

2. Device Structures and Experimental Details

A conventional plasma-enhanced chemical vapor deposition (PECVD) system was used to deposit a-Si/a-SiC multilayers at the substrate temperature of 250 °C. The a-Si layer was prepared by using silane (SiH_4) gas, and the thickness was controlled at 4 nm while the a-SiC layer with thickness of 2 nm was prepared by using gas mixture of $SiHS_4$ and methane (CH_4) with a gas ratio of $(CH_4/SiH_4) = 10$. The total period is 20. Part of the samples deposited on p-Si substrate (1–3 Ωcm) was successively deposited by Phosphorous-doped a-Si layer ($\sim$10 nm) as an n-type contact layer. This n-layer was deposited by gas mixture of PH_3 (1% in H_2) and SiH_4 with the ratio of $(PH_3/SiH_4) = 10$. It is found that the device properties get worse when we take a much higher phosphorus concentration to get a better conductive performance. The reference sample without the p-i-n structure was also prepared, which has only multilayers deposited on p-Si substrate. After deposition of samples, a KrF pulsed excimer laser (248 nm, 30 ns) was used to crystallize the a-Si layer to form Si QDs. A single pulse was used, and the laser fluence is ranged from 0 to 183 mJ/cm^2, and the irradiation area is about 1 cm^2. Finally, an Aluminum electrode was evaporated on the rear side of the p-Si substrate, and a transparent Indium-Tin-Oxide (ITO) electrode was used on the top side to get the EL device, as shown in Fig. 1.

3. Results and Discussion

Fig. 2 shows the cross-sectional transmission electron microscopy (TEM) image of prepared Si QDs/SiC MLs after laser crystallization. It is clearly shown that the periodic structure is still kept even after laser irradiation, and the thickness of each layer is in well agreement with the pre-designed value. The formation of Si QDs in a-Si layers can be identified in the high-resolution TEM image, as given in the inset in Fig. 1. The average size of the Si QDs is about 4 nm, which reflects
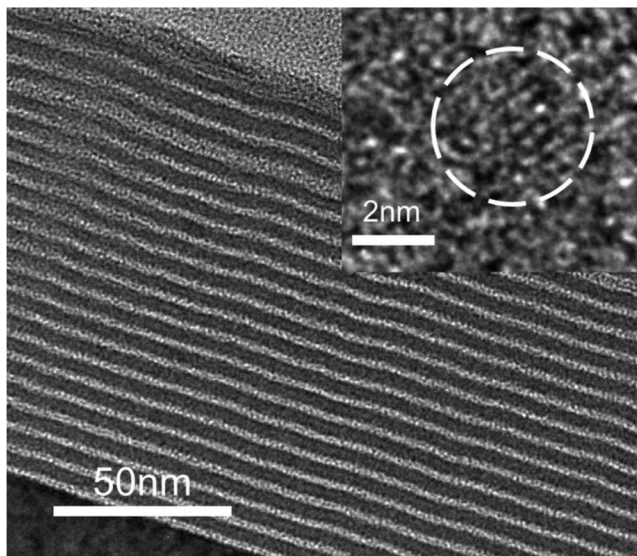
Fig. 2. Cross-sectional TEM image of the multilayer structure, inset indicates the formation of Si QDs after laser crystallization.
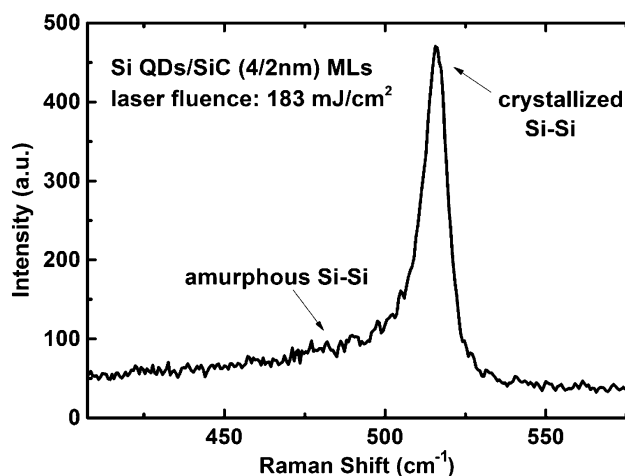

Fig. 3. Raman spectra of Si QDs/SiC multilayers embedded in p-i-n structure on quartz substrate under the energy fluence of 183 mJ/cm^2.

the constrained crystallization in the multilayer structure, as reported in our previous works [17], [18]. It is found that the a-Si layer starts to be crystallized when the laser fluence is higher than 150 mJ/cm^2, and the crystallinity is gradually increased with increasing the laser fluence. As given in Fig. 3, an intense and sharp band appears in the Raman spectrum ($\sim$516 cm^{-1}) for Si QDs/SiC MLs after laser crystallization with fluence of 183 mJ/cm^2. It is indicated that the a-Si layer is crystallized. It is worth noting *that* the a-SiC layer is quite stable both under the high-temperature annealing and laser annealing process, and the weak Raman band centered at 480 cm^{-1} as shown in Fig. 3 may be associated with the a-Si phase in SiC layers.

The current–voltage ($I-V$) relationship of the p-i-n device is investigated and compared with the reference sample without the p-i-n structure. As shown in Fig. 4, the device with the p-i-n structure exhibits a good rectification characteristic. The reverse current is on the order of 10^{-7} A, which is obviously reduced by three orders of magnitude compared with that of reference sample
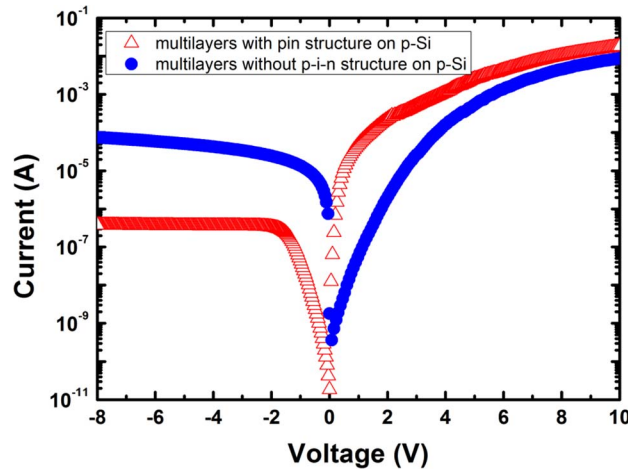
Fig. 4. Current–voltage curves of both Si QDs/SiC multilayers embedded in p-i-n structure and the reference device with only Si QDs/SiC multilayer structure on p-type crystalline silicon.
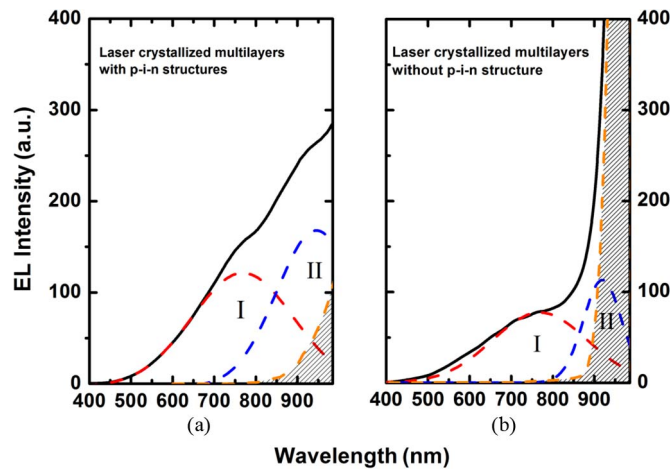

Fig. 5. EL intensity of p-i-n structure (a) compared with MLs structure (b) under the same voltage of 10 V, the dash lines are peaks divided from the original emission line.

($> 10^{-4}$ A). The I_{on}/I_{off} ratio of the prepared p-i-n device at voltage of ± 6 V is larger than 10^4, which suggests the formation of a good p-i-n junction containing Si QDs/SiC MLs using the present approach.

Fig. 5 shows the room temperature EL spectra for the p-i-n device and the reference sample at the applied bias of 10 V. A broad EL band is observed, and the EL intensity of the p-i-n device is enhanced compared with that of the reference sample. The EL spectrum can be divided into two sub-bands, which are located at 750 nm and 930 nm, respectively. The 750-nm emission can be attributed to the recombination of electron–hole pairs in Si QDs. G. R. Lin *et al.* pointed out that the band-to-band transition energies of first-order excited states for a nc-Si QD with the diameter of 4 nm are calculated as $E_1 = 1.64$ eV ($\lambda = 756$ nm), which is well in agreement with the emission peak energy of band I observed in our case [19]. However, the EL spectrum exhibits a relatively long wavelength, which may due to the size deviation, and some of the Si-QD size could be larger than 4–5 nm. The 930-nm emission can be explained as the recombination via interface states or the band tail states of a-SiC [20]–[22]. The remaining shadowed part in the infrared region can be ascribed to the band-edge emission of the Si substrate [21]. The EL device performance can be further evaluated by estimating the luminescence efficiency. We calculated the ratio of integrated
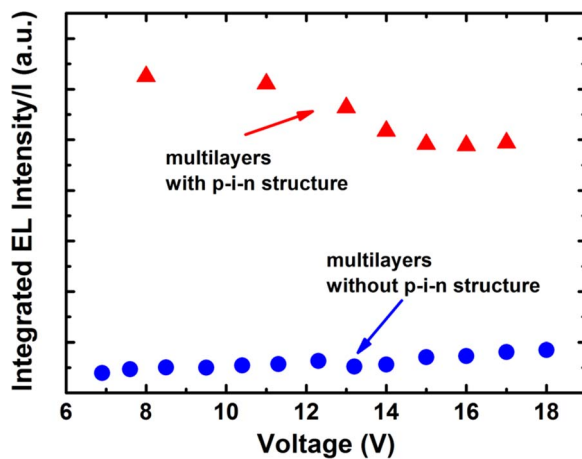
Fig. 6. The ratio of integrated EL intensity to injection current of EL device with and without p-i-n structure.
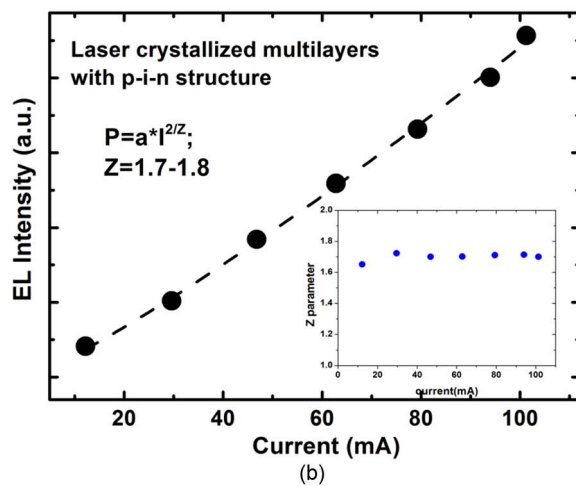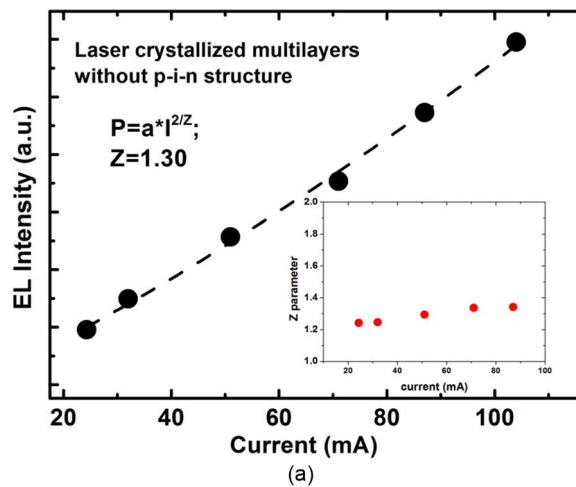

Fig. 7. EL intensity of device based on Si QDs/SiC MLs without (a) and with (b) p-i-n structure as a function of injection current. The corresponding Z parameter of each device is shown in the inset in each figure.

EL intensity to the injection current at a given voltage, which can reflect the device luminescence efficiency. As given in Fig. 6, it is clearly seen that the emission efficiency is 5–10 times higher than that of the reference sample in the measurement range.

The improved device performance can be attributed to the increased radiative recombination probability of electron–hole pairs by forming the p-i-n junction. In order to further understand the recombination process of injected carriers, the relationship between the EL intensity and injection current is studied both for devices with and without the p-i-n structure. It is known that the current can be expressed as $I = N^Z (1 < Z < 3)$, where N is the carrier concentration, and Z is a power index. $Z = 1, 2$, and 3 stands for the recombination of carriers via defect states, radiative, and Auger process, respectively [21], [23]. Taking into account that the EL intensity P_{EL} is proportional to the radiative recombination of electron–hole pairs, $P_{EL} \sim N^2$, one can get $P_{EL} \sim I^{2/z}$. Therefore, by plotting the power relationship of EL intensity P_{EL} as a function of current I, the Z parameter can be deduced. The dependence of EL intensity on the current of the p-i-n device and the reference sample is shown in Fig. 7(a) and (b), and the deduced Z-parameter is given in the inset in Fig. 7. It is found that the Z-parameter is 1.3 for the reference sample, and it is increased to 1.7–1.8 for p-i-n EL devices, which suggests that both the defect-related and radiated recombination processes are involved in our device, but the Auger recombination process can be negligible. The Z-parameter was also studied in SiO_x:Si-QD light-emitting devices previously. The Z parameter data in our case are very close to 2, whereas the obtained value in the SiO_x:Si-QD case is 2–3, which indicated that Auger recombination becomes dominant under high bias by using the SiO_x matrix [24]. We contribute our advantage to the SiC host matrix in two aspects. Firstly, the SiC matrix has a lower potential barrier compared with the SiO_x matrix, which makes it easier for the current injunction. Secondly, a better thermal dissipation of the SiC host matrix could contribute to the result in a large extent. The increased Z-parameter indicates that radiative recombination dominates the recombination process of injected carriers in the p-i-n device, which can explain the improvement of device performance.

4. Conclusion

In summary, we have reported the p-i-n structure EL device prepared by laser crystallization with Si QDs/SiC multilayers embedded. It was found that the diffusion of impurities can be restrained and that the structure remains well after laser irradiation. Moreover, we found out that the recombination process of electrons and holes was enhanced within the p-i-n structure by establishing the Z-parameter model, which results in enhancing the emission efficiency 5–10 times higher than that of the reference sample without the p-i-n structure.

References

[1] N. Daldosso and L. Pavesi, "Nanosilicon Photonics," *Laser Photon. Rev.*, vol. 3, no. 6, pp. 508–534, Nov. 2009.

[2] B. H. Lai, C. H. Cheng, and G. R. Lin, "Multicolor ITO/SiO$_x$/p-Si/Al light emitting diodes with improved emission efficiency by small Si quantum dots," *IEEE J. Quantum Electron.*, vol. 47, no. 5, pp. 698–704, May 2011.

[3] X. Wang, R. Huang, C. Song, Y. Q. Guo, and J. Song, "Effect of barrier layers on electroluminescence from Si/SiO$_x$N$_y$ multilayer structures," *Appl. Phys. Lett.*, vol. 102, no. 8, pp. 081114-1–081114-4, Feb. 2013.

[4] A. Anopchenko, A. Marconi, E. Moser, L. Pavesi, G. Pucker, and P. Bellutti, "Low-voltage onset of electroluminescence in nanocrystalline-Si/SiO$_2$ multilayers," *J. Appl. Phys.*, vol. 106, no. 3, pp. 033104-1–033104-8, Aug. 2009.

[5] H. Y. Tai, Y. H. Lin, and G. R. Lin, "Wavelength-shifted yellow electroluminescence of si quantum-dot embedded 20-pair SiNx/SiOx superlattice by ostwald ripening effect," *IEEE J. Photon.*, vol. 5, no. 1, p. 6600110, Feb. 2013.

[6] J. Zhou, G. R. Chen, Y. Liu, and J. Xu, "Electroluminescent devices based on amorphous SiN/Si quantum dots/amorphous SiN sandwiched structures," *Opt. Exp.*, vol. 17, no. 1, pp. 156–162, Jan. 2009.

[7] Y. J. Rui, S. X. Li, Y. Q. Cao, J. Xu, W. Li, and K. J. Chen, "Structural and electroluminescent properties of Si quantum dots/SiC multilayers," *Appl. Surf. Sci.*, vol. 269, pp. 37–40, Mar. 2013.

[8] C. H. Cheng, C. L. Wu, C. C. Chen, L. H. Tsai, Y. H. Lin, and G. R. Lin, "Si-rich Si$_x$C$_{1-x}$ light-emitting diodes with buried si quantum dots," *IEEE J. Photon.*, vol. 4, no. 5, pp. 1762–1775, Oct. 2012.

[9] H. Takami, K. Makihara, M. Ikeda, and S. Miyazaki, "Characterization of electroluminescence from one-dimensionally self-aligned si-based quantum dots," *Jpn. J. Appl. Phys*, vol. 52, p. 04CG08, Apr. 2013.

[10] O. Jambois, H. Rinnert, X. Devaux, and M. Vergnat, "Photoluminescence and electroluminescence of size-controlled silicon nanocrystallites embedded inSiO$_2$ thin films," *J. Appl. Phys.*, vol. 98, no. 4, pp. 046105-1–046105-3, Aug. 2005.

[11] N. M. Park, T. S. Kim, and S. J. Park, "Band gap engineering of amorphous silicon quantum dots for light-emitting diodes," *Appl. Phys. Lett.*, vol. 78, no. 17, pp. 2575–2577, Apr. 2001.

[12] Y. Rui, S. Li, J. Xu, C. Song, X. Jiang, W. Li, W. Chen, Q. Wang, and Y. Zuo, "Size-dependent electroluminescence from Si quantum dots embedded in amorphous SiC matrix," *J. Appl. Phys.*, vol. 110, no. 6, pp. 064322-1–064322-6, Sep. 2011.

[13] C. L. Wu and G. R. Lin, "Power gain modeling of si quantum dots embedded in a SiOx waveguide amplifier with inhomogeneous broadened spontaneous emission," *IEEE J. Select. Topics Quantum Electron.*, vol. 19, no. 5, pp. 1–9, Sep./Oct. 2013.

[14] D. Y. Chen, D. Y. Wei, J. Xu, P. G. Han, X. Wang, Z. Y. Ma, K. J. Chen, W. H. Shi, and Q. M. Wang, "Enhancement of electroluminescence in p–i–n structures with nano-crystalline Si/SiO_2 multilayers," *Semicond. Sci. Technol.*, vol. 23, no. 1, p. 015013, Jan. 2008.

[15] J. S. Huang, P. Martin, W. Ansgar, B. Jan, L. Karl, and S. Y. Liu, "Low-voltage organic electroluminescent devices using pin structures," *Appl. Phys. Lett.*, vol. 80, no. 1, pp. 139–141, Jan. 2002.

[16] I. Perez-Wurfl, L. Ma, D. Lin, X. Hao, M. A. Green, and G. Conibeer, "Silicon nanocrystals in an oxide matrix for thin film solar cells with 492mV open circuit voltage," *Sol. Energy Mater. Sol. Cells*, vol. 100, pp. 65–68, May 2012.

[17] G. R. Chen, J. Xu, W. Xu, H. C. Sun, W. W. Mu, S. H. Sun, Z. Y. Ma, X. F. Huang, and K. J. Chen, "Dynamical process of KrF pulsed excimer laser crystallization of ultrathin amorphous silicon films to form Si nano-dots," *J. Appl. Phys.*, vol. 111, no. 9, pp. 094320-1–094320-5, May 2012.

[18] M. X. Wang, K. J. Chen, L. He, W. Li, J. Xu, and X. F. Huang, "Green electro- and photoluminescence from nanocrystalline Si film prepared by continuous wave Ar^+ laser annealing of heavily phosphorus doped hydrogenated amorphous silicon film," *Appl. Phys. Lett.*, vol. 73, no. 1, pp. 105–107, Jul. 1998.

[19] G. R. Lin, C. J. Lin, C. K. Lin, L. J. Chou, and Y. L. Chueh, "Oxygen defect and Si nanocrystal dependent white-light and near-infrared electroluminescence of Si-implanted and plasma-enhanced chemical-vapor deposition-grown Si-rich SiO2," *J. Appl. Phys.*, vol. 97, no. 9, pp. 094306-1–094306-8, May 2005.

[20] Z. Wang, V. Suendo, A. Abramov, L. W. Yu, and P. Roca i Cabarrocas, "Strongly enhanced tunable photoluminescence in polymorphous silicon carbon thin films via excitation-transfer mechanism," *Appl. Phys. Lett.*, vol. 97, no. 22, pp. 221113-1–221113-3, Nov. 2010.

[21] W. W. Mu, P. Zhang, J. Xu, S. H. Sun, J. Xu, W. Li, and K. J. Chen, "Direct-current and alternating-current driving si quantum dots-based light emitting device," *IEEE J. Select. Topics Quantum Electron.*, vol. 20, no. 4, pp. 8 200 106–8 200 107, Jul./Aug. 2014.

[22] K. Dusit, E. Toshihito, G. P. Wei, O. Hiroaki, and H. Yoshihiro, "Visible-light injection-electroluminescent a-SiC/p-i-n diode," *Jpn. J. Appl. Phys.*, vol. 24, no. 2, pp. L806–L808, Oct. 1985.

[23] R. Fehse, S. Tomic, A. R. Adams, S. J. Sweeney, E. P. OReilly, A. Andreev, and H. Riechert, "A Quantitative study of radiative, auger, and defect related recombination processes in 1.3-μm GaInNAs-based quantum-well lasers," *IEEE J. Select. Topics Quantum Electron.*, vol. 8, no. 4, pp. 801–810, Jul./Aug. 2002.

[24] C. H. Cheng, Y. C. Lien, C. L. Wu, and G. R. Lin, "Mutlicolor electroluminescent Si quantum dots embedded in $SiOS_x$ thin film MOSLED with 2.4% external quantum efficiency," *Opt. Exp.*, vol. 21, no. 1, pp. 391–403, Jan. 2013.